

Search for Light Gauge Bosons of the Dark Sector at the Mainz Microtron

H. Merkel,^{1,*} P. Achenbach,¹ C. Ayerbe Gayoso,¹ J. C. Bernauer,^{1,†} R. Böhm,¹ D. Bosnar,² L. Debenjak,³ A. Denig,¹ M. O. Distler,¹ A. Esser,¹ H. Fonvieille,⁴ I. Friščić,² D. G. Middleton,¹ U. Müller,¹ L. Nungesser,¹ J. Pochodzalla,¹ M. Rohrbeck,¹ S. Sánchez Majos,¹ B. S. Schlimme,¹ M. Schoth,¹ S. Širca,^{3,5} and M. Weinriefer¹

(A1 Collaboration)

¹*Institut für Kernphysik, Johannes Gutenberg-Universität Mainz, D-55099 Mainz, Germany*[‡]

²*Department of Physics, University of Zagreb, HR-10002 Zagreb, Croatia*

³*Jožef Stefan Institute, SI-1000 Ljubljana, Slovenia*

⁴*Clermont Université, Université Blaise Pascal, CNRS/IN2P3, LPC, BP 10448, F-63000 Clermont-Ferrand, France*

⁵*Department of Physics, University of Ljubljana, SI-1000 Ljubljana, Slovenia*

(Received 21 January 2011; published 22 June 2011)

A new exclusion limit for the electromagnetic production of a light $U(1)$ gauge boson γ' decaying to e^+e^- was determined by the A1 Collaboration at the Mainz Microtron. Such light gauge bosons appear in several extensions of the standard model and are also discussed as candidates for the interaction of dark matter with standard model matter. In electron scattering from a heavy nucleus, the existing limits for a narrow state coupling to e^+e^- were reduced by nearly an order of magnitude in the range of the lepton pair mass of $210 \text{ MeV}/c^2 < m_{e^+e^-} < 300 \text{ MeV}/c^2$. This experiment demonstrates the potential of high current and high resolution fixed target experiments for the search for physics beyond the standard model.

DOI: 10.1103/PhysRevLett.106.251802

PACS numbers: 14.70.Pw, 25.30.Rw, 95.35.+d

Introduction.—An additional $U(1)$ interaction appears to be natural in nearly all theoretical extensions of the standard model. Large gauge symmetries have to be broken, and $U(1)$ bosons provide the lowest-rank local symmetries. For example, in standard embedding of most variants of string theories, a $U(1)$ boson is generated by symmetry breaking. Such additional $U(1)$ bosons may be hidden; e.g., no standard model particles are charged under the corresponding symmetry, but their mass is allowed in the range of the standard model masses.

Recently, several experimental anomalies were discussed as possible signatures for a hidden force. A light $U(1)$ boson in the mass range below $1 \text{ GeV}/c^2$ might explain, e.g., the observed anomaly of the muon magnetic moment [1,2]. Cosmology and astrophysics provide an abundant amount of evidence for the existence of dark matter (for a summary, see, e.g., Ref. [3]). Several experimental hints point to a $U(1)$ boson coupling to leptons as the mediator of the interaction of dark matter with standard model matter (see, e.g., Ref. [4] for a detailed discussion). For example, the lively debated annual modulation signal of the DAMA-LIBRA experiment [5] could be brought into accordance with the null result of bolometric experiments if one assumes an interaction via a light $U(1)$ boson [6]. Observations of cosmic rays show a positron excess [7]. While this excess may be due to astrophysical process like quasars, this could also be a hint for the annihilation of dark matter into leptons. If the experimental evidence is interpreted as annihilation of dark matter, the excess of positrons and no excess of

antiprotons in cosmic rays hints again to a mass of the $U(1)$ boson below $2 \text{ GeV}/c^2$.

The interaction strength of such a $U(1)$ boson (in the following denoted as γ' , in the literature also denoted as A' , U , or ϕ) with standard model particles is governed by the mechanism of kinetic mixing [8]. The coupling can be subsumed by an effective coupling constant ϵ and a vertex structure of a massive photon.

Bjorken *et al.* [9] discussed several possible experimental schemes for the search of a γ' in the most likely mass range of a few MeV/c^2 up to a few GeV/c^2 . Since the coupling is small, the cross section for coherent electromagnetic production of the γ' boson can be enhanced by a factor Z^2 by choosing a heavy nucleus as the target (see Fig. 1). The subsequent decay of the γ' boson to a lepton pair is the signature of the reaction.

The cross sections of signal and background were estimated in Ref. [9] in the Weizsäcker-Williams approximation. In this approximation, the cross section shows a sharp

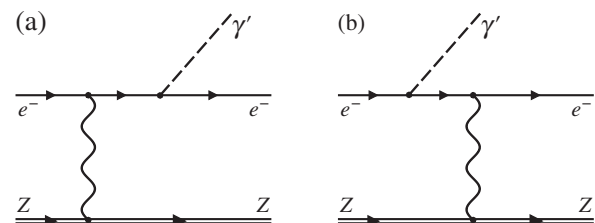


FIG. 1. Electromagnetic production of the γ' boson. The coupling of the γ' boson is parametrized as $i\epsilon e\gamma^\mu$.

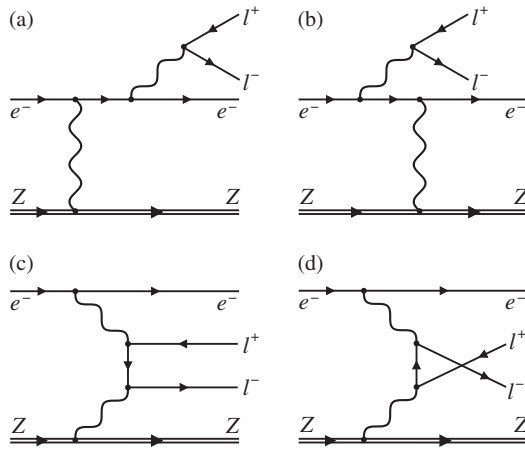


FIG. 2. Dominant background processes. While graphs (a) and (b) have the same structure as the signal and present an irreducible background, the contributions of graphs (c) and (d) can be suppressed by the choice of kinematic setting.

peak, in both signal and background, where nearly all the energy of the incident electron is transferred to the lepton pair ($E_{e^+} + E_{e^-} = E_0$). Correspondingly, the pair is produced dominantly in the direction of the incident electron.

The experimental challenge is the suppression of the background, which is dominated by radiative pair production (Fig. 2). Radiation by the final or initial electron [Figs. 2(a) and 2(b)] has the same cross-section structure as the desired signal and is an irreducible background to this experiment. Radiation with an internal lepton line [Figs. 2(c) and 2(d)] has a maximum if the internal electron line is nearly on the mass shell, i.e., if one of the leptons carries nearly all the energy of the pair. This background can be reduced by choosing a kinematic setting in which the electron and positron are detected at equal angles and momenta.

Experiment.—The experiment took place at the spectrometer setup of the A1 Collaboration at the Mainz Microtron (MAMI) (see Ref. [10] for a detailed description). An unpolarized electron beam with a beam energy of $E_0 = 855$ MeV and a beam current of $90 \mu\text{A}$ was incident on a tantalum foil (99.9% ^{181}Ta , $Z = 73$) with an area density of 81.3 mg/cm^2 , leading to a luminosity of $LZ^2 = 8.07 \times 10^{38} \text{ s}^{-1} \text{ cm}^{-2}$. The beam was rastered across the target to reduce the local thermal load on the target foil.

For the detection of the electron-positron pair, two high-resolution spectrometers were used. The particles were

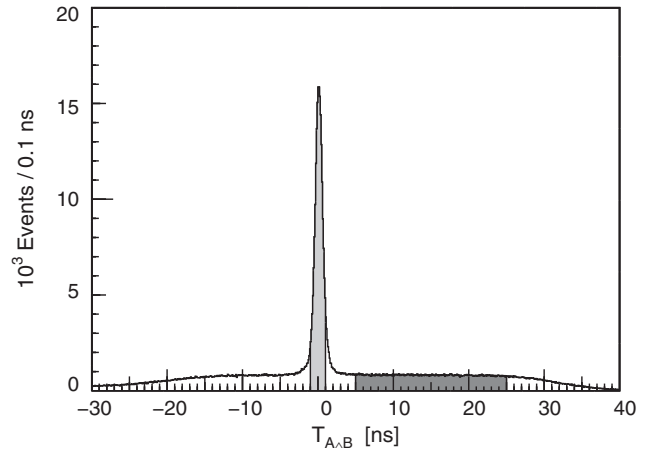


FIG. 3. Coincidence time distribution after particle identification by Čerenkov detectors (setup 1). The events of the light shaded area were used as true coincidences, while the dark shaded area was used as an estimate of the accidental coincidences.

detected by vertical drift chambers for tracking and scintillator detectors for trigger and timing purposes. In addition, a threshold-gas-Čerenkov detector was used in each arm to discriminate between electrons or positrons and pions.

Table I summarizes the kinematic setups used. Setup 1 was chosen to be close to $E_{e^+} + E_{e^-} = E_0$, where the cross section has a sharp peak to ensure high count rates. In addition, setup 2 was selected at $E_{e^+} + E_{e^-} = 0.9E_0$ during the experiment to optimize the total count rates. The angles of the spectrometers were set to be nearly symmetric to reduce the background by the Bethe-Heitler process [Figs. 2(c) and 2(d)]. In total, data of four days of beam time were used for the analysis. The electrons and the positrons were detected by the coincidence of the raw scintillator signals. The Čerenkov signals were not included in the trigger logic but recorded for off-line analysis.

Data analysis.—Only events with a positive signal in the Čerenkov detectors were selected with an efficiency of 98% for spectrometer A and 95% for spectrometer B [10]. Figure 3 shows the coincidence time between the corresponding spectrometers after correction for the flight path of ≈ 12 m within the spectrometers for these events. A timing resolution of better than 1 ns FWHM was achieved, and a cut of $-1 \text{ ns} < t_{A \wedge B} < 1 \text{ ns}$ was used to mark the true electron-positron pairs. Below the peak, a

TABLE I. Kinematic settings. The incident beam energy was $E_0 = 855$ MeV, and the settings are roughly centered around $E_{e^+} + E_{e^-} = E_0$ and $m_\gamma = 250 \text{ MeV}/c^2$.

	Spec. A (e^+)			Spec. B (e^-)			Events
	p (MeV)	θ	$d\Omega$ (msr)	p (MeV)	θ	$d\Omega$ (msr)	
Setup 1	346.3	22.8°	21	507.9	15.2°	5.6	208×10^6
Setup 2	338.0	22.8°	21	469.9	15.2°	5.6	47×10^6

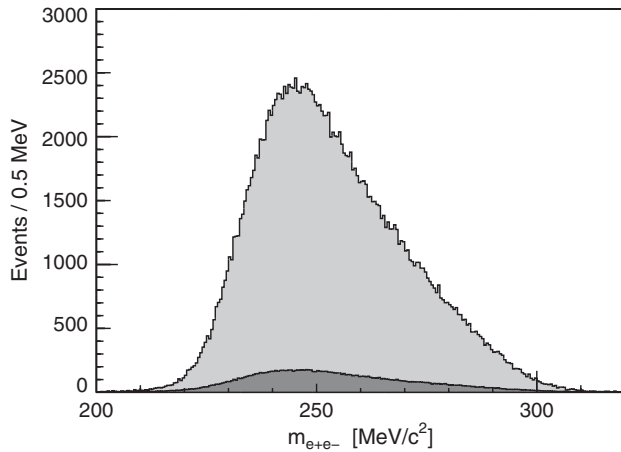


FIG. 4. Mass distribution of the reconstructed e^+e^- pair (setup 1). The dark shaded area denotes the background due to accidental coincidences (scaled to a time window of 2 ns).

background due to accidental coincidences is present. To estimate this background, events in the coincidence side band $5 \text{ ns} < t_{A \wedge B} < 25 \text{ ns}$ were selected and weighted by the ratio of the timing windows.

For the real electron-positron pairs, the invariant mass squared of the pair was determined by the four-momentum sum $m_{e^+e^-}^2 = (p_{e^+} + p_{e^-})^2$. Figure 4 shows the resulting mass spectrum. The contribution of the accidental background is indicated by the dark shaded area.

In this figure, a possible candidate for the dark photon would appear as a peak on top of the background. The width of such a peak can only be estimated by simulation. For this, the experimental resolution of the four-vector determination of a single spectrometer was determined by the width of the lowest lines of the nuclear excitation spectrum in elastic electron scattering. This single spectrometer resolution was used as input for the simulation of the experiment. A mass resolution of better than $0.5 \text{ MeV}/c^2$ was determined, corresponding to the chosen bin width in Fig. 4.

No significant peak in the mass spectrum was observed. The corresponding upper limit was determined by the Feldman-Cousins algorithm [11]. As input for this algorithm the raw mass spectrum was used, and as a background estimate for each bin the mean of the three neighboring bins on either side was used. This choice of the background estimate introduces systematic errors, which have to be investigated in the case of a positive signal but only enhance statistical fluctuations in the case of an upper limit. Figure 5 shows the resulting exclusion limits.

Results and interpretation.—In order to interpret the result in terms of the effective coupling ϵ of a possible dark photon candidate, a model for the production process has to be used. Unfortunately, it turns out that the Weizsäcker-Williams approximation used in Ref. [9] fails in this energy range by orders of magnitude, mainly since the recoil of the nucleus cannot be neglected. Taking into account the nuclear recoil, the peak at $(E_{e^+} + E_{e^-}) = E_0$ in Ref. [9] is regularized, and the cross section at this point becomes zero. In addition, the assumption of a real initial photon exactly in the direction of the electron beam introduces a peak in the angular distribution, which is not present in electroproduction due to helicity conservation of the scattered electron.

Instead, we used as a model for the γ' production the coherent electroproduction from the tantalum nucleus, calculated as the coherent sum of the graphs of Fig. 1. The charge distribution of tantalum was approximated as a solid sphere. For the QED background we used the coherent sum of the graphs of Fig. 2. The corresponding cross sections were included on an event by event basis in the simulation. The simulation including this model shows excellent agreement with data, as demonstrated in Fig. 6, where the background-subtracted yields as an estimate for the QED background graphs are compared to the simulation of this process.

The remaining model dependence of this interpretation mainly affects the nuclear vertex, since, e.g., the possible

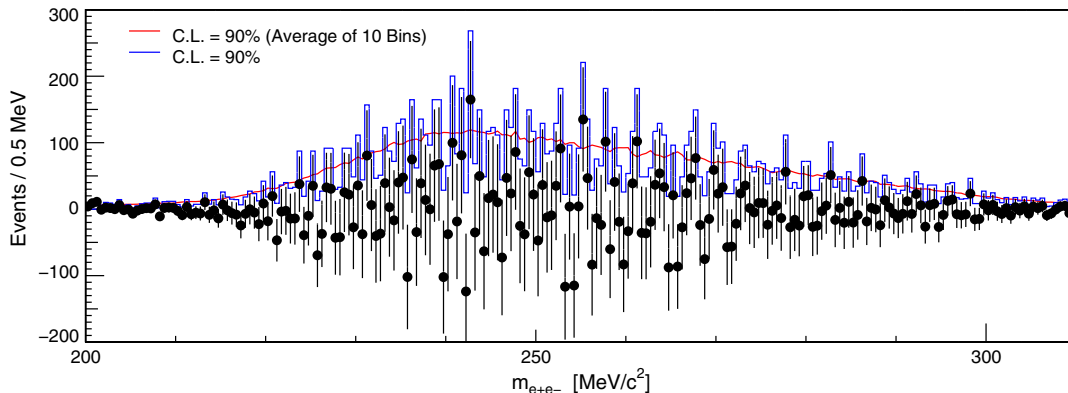


FIG. 5 (color online). Upper exclusion limits with 90% confidence level determined by the Feldman-Cousins algorithm (all data). The averaged limit is included for subjective judgement only ($\approx 10\%$ of the data points should be above this line at 90% C.L.).

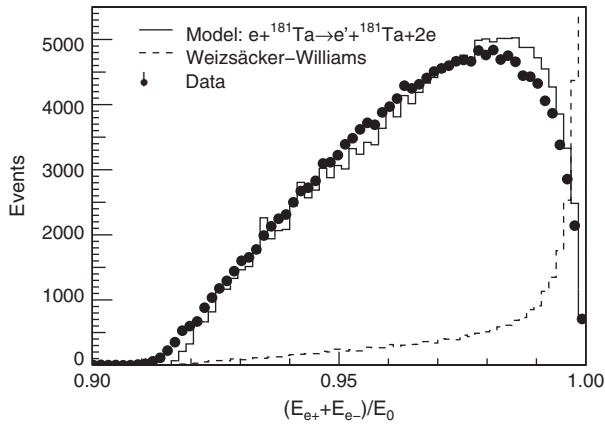


FIG. 6. Comparison of simulation with data (setup 1). As a model the coherent electroproduction from a heavy nucleus was used.

breakup of the recoil nucleus is neglected. Since this vertex is common to both the signal and the QED background channels, to further reduce the model dependence we use only the ratio of the signal to QED background of the simulation in addition to the accidental background. The ratio can be translated to the effective coupling for a given mass resolution δ_m by using Eq. (19) of Ref. [9]:

$$\frac{d\sigma(X \rightarrow \gamma' Y \rightarrow e^+ e^- Y)}{d\sigma(X \rightarrow \gamma^* Y \rightarrow e^+ e^- Y)} = \frac{3\pi}{2N_f} \frac{\epsilon^2}{\alpha} \frac{m_{\gamma'}}{\delta_m}$$

and the measured event rate as an estimate for the background channel. The number of final states N_f includes the ratio of phase space for the corresponding decays above the $\mu^+ \mu^-$ threshold.

Figure 7 shows the result of this experiment in terms of the ratio of the effective coupling to the fine structure constant $\alpha'/\alpha = \epsilon^2$. For clarity of the figure, the exclusion limit was averaged. Also shown are the existing limits published by *BABAR* [12] and the standard model prediction [2] of the muon anomalous magnetic moment $a_\mu = g_\mu/2 - 1$ (calculation of exclusion limits in ϵ^2 by [13]). The existing exclusion limit has been extended by an order of magnitude.

In this experiment, the discovery potential of the existing high luminosity electron accelerators has been demonstrated. The background conditions are well under control due to excellent timing and missing mass resolution. An extensive program to cover further mass regions with similar experiments is planned at MAMI, Jefferson Lab [13], and other laboratories (for a review, see Ref. [14]).

The authors thank the MAMI accelerator group for providing the excellent beam quality and intensity necessary for this experiment and T. Beranek for fruitful discussions on the QED calculations. This work was

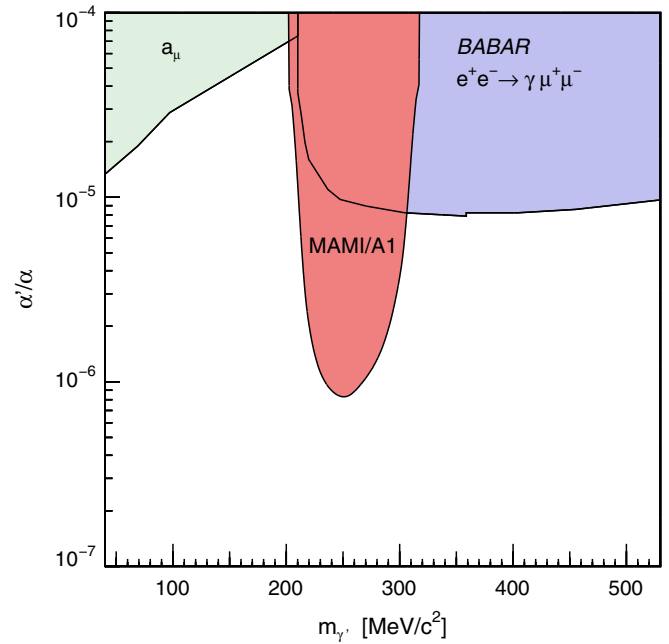


FIG. 7 (color online). Exclusion limits with 90% confidence level in terms of relative coupling $\alpha'/\alpha = \epsilon^2$. Also shown are the previous results by *BABAR* [12] and for a_μ of the muon [2].

supported by the Federal State of Rhineland-Palatinate and by the Deutsche Forschungsgemeinschaft with the Collaborative Research Center 443.

*merkel@kph.uni-mainz.de

†Present address: MIT-LNS, Cambridge, MA, USA.

‡http://www.kph.uni-mainz.de

- [1] G. W. Bennett *et al.*, *Phys. Rev. D* **73**, 072003 (2006).
- [2] M. Pospelov, *Phys. Rev. D* **80**, 095002 (2009).
- [3] K. Nakamura *et al.* (Particle Data Group), *J. Phys. G* **37**, 075021 (2010).
- [4] N. Arkani-Hamed, D. P. Finkbeiner, T. R. Slatyer, and N. Weiner, *Phys. Rev. D* **79**, 015014 (2009).
- [5] R. Bernabei *et al.*, *Eur. Phys. J. C* **56**, 333 (2008).
- [6] N. Borodatchenkova, D. Choudhury, and M. Drees, *Phys. Rev. Lett.* **96**, 141802 (2006).
- [7] O. Adriani *et al.*, *Nature (London)* **458**, 607 (2009).
- [8] B. Holdom, *Phys. Lett.* **166B**, 196 (1986).
- [9] J. D. Bjorken, R. Essig, P. Schuster, and N. Toro, *Phys. Rev. D* **80**, 075018 (2009).
- [10] K. I. Blomqvist *et al.*, *Nucl. Instrum. Methods Phys. Res., Sect. A* **403**, 263 (1998).
- [11] G. J. Feldman and R. D. Cousins, *Phys. Rev. D* **57**, 3873 (1998).
- [12] B. Aubert *et al.*, *Phys. Rev. Lett.* **103**, 081803 (2009).
- [13] R. Essig, P. Schuster, N. Toro, and B. Wojtsekhowski, *J. High Energy Phys.* **02** (2011) 009.
- [14] S. Andreas and A. Ringwald, arXiv:1008.4519.